Hole doping of mechanically exfoliated graphene by confined hydration layers

Tjeerd R. J. Bollmann[1,2](✉), Liubov Yu. Antipina[3,4], Matthias Temmen[2], Michael Reichling[2], Pavel B. Sorokin[5]

Just Accepted

Hole doping of mechanically exfoliated graphene by confined hydration layers

Tjeerd R.J. Bollmann*, Liubov Y. Antipina, Matthias Temmen, Michael Reichling, Pavel B. Sorokin

MESA+ Institute for Nanotechnology, The Netherlands
Universität Osnabrück, Germany
Moscow Institute of Physics and Technology, Russian Federation
Siberian Federal University, Russian Federation
National University of Science and Technology MISiS, Russian Federation
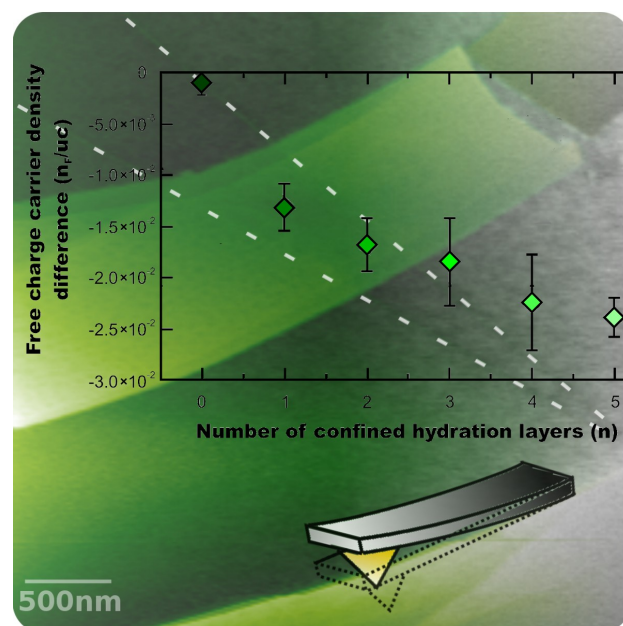
In this paper, we investigate the water layers that are confined during mechanical exfoliation and electronically modify the graphene as electron-density from the graphene is transferred towards this hydration layer. We combine experimental state-of-the-art observations using non-contact Atomic Force Microscopy (NC-AFM) and Kelvin Probe Force Microscopy (KPFM) together with Molecular Dynamics (MD) and Density Functional Theory (DFT) calculations to identify the electronic contributions of the different hydration layer thicknesses to graphene.

Hole doping of mechanically exfoliated graphene by confined hydration layers

Tjeerd R. J. Bollmann[1,2](✉), Liubov Yu. Antipina[3,4], Matthias Temmen[2], Michael Reichling[2], Pavel B. Sorokin[5]

[1]*Inorganic Materials Science, MESA+ Institute for Nanotechnology, P.O. Box 217, 7500AE Enschede, The Netherlands*
[2]*Fachbereich Physik, Universität Osnabrück, Barbarastraße 7, 49076 Osnabrück, Germany*
[3]*Moscow Institute of Physics and Technology, Dolgoprudny, 141700, Russian Federation*
[4]*Siberian Federal University, Krasnoyarsk, 660041, Russian Federation*
[5]*National University of Science and Technology MISiS, Moscow, 119049, Russian Federation*

ABSTRACT

By the use of non-contact Atomic Force Microscopy (NC-AFM) and Kelvin Probe Force Microscopy (KPFM), we measure the local surface potential of graphene mechanically exfoliated on $CaF_2(111)$ as a prototype insulating surface. The hydration layers confined between graphene and substrate, resulting from preparation under ambient conditions on the hydrophilic surface are found to electronically modify the graphene as electron-density is transferred from graphene to the hydration layer. Density Functional Theory (DFT) calculations predict that the first 2 to 3 water layers adjacent to the graphene hole dope graphene by several percent of a unit charge per unit cell.

Introduction

The demonstration of two-dimensional electronic properties in mechanically exfoliated graphene[1] has resulted in tremendous interest of investigating the unique properties of this and various other 2D materials. In comparison to other preparation methods, mechanical exfoliation of graphene on a substrate results in flakes of high quality[1,2]. The ambient conditions present during such preparation, however, result in rather uncontrolled electronic properties of 2D materials[3]. This is due to the capture of thin water layers resulting from moist in the atmosphere[4–12]. Confined water layers have been described as modifying the electronic properties of the graphene, as they are thought to effectively shield the interfacial charge on (electrically insulating) substrates[10]. A negative surface charge has been reported for 'electroneutral' mica substrates to be caused by the confined water layer and has been suggested to result in doped graphene. The mechanism of electronic modification by confined water between substrate and exfoliated graphene, however, is not yet well understood[10,13].

Here, we study the electronic properties of mechanically exfoliated graphene confining hydration layers (HLs) that result from the preparation under ambient conditions on a prototype insulating hydrophilic substrate, namely $CaF_2(111)$. Using non-contact Atomic Force Microscopy (NC-AFM) and Kelvin Probe Force Microscopy (KPFM), we investigate modifications of the surface potential due to the partial removal of HLs upon heating. To investigate the origin of the electronic modification of graphene by different HL thicknesses, we compare experimentally obtained topography and KPFM measurements to a quantitave model calculated by density functional theory (DFT). Our observations demonstrate the role of charge transfer between the HLs and graphene in the modification of its electronic properties.

Experimental

Graphene is mechanically exfoliated[1] under ambient conditions from an HOPG crystal onto a $CaF_2(111)$ substrate cleaved under similar conditions shortly before[12]. The resulting graphene flakes are inspected before insertion into an ultra-high vacuum chamber (UHV) by an optical microscope. As an indication for the graphene flakes thickness in general, we characterized the thickness of graphene flakes beyond the available spotsize by Raman microscopy using the G and 2D bands[14,15]. Prior to the NC-AFM measurements, the sample is heated under UHV conditions (base pressure below 1×10^{-10} mbar) to 400 K to partially remove the thicker HLs[12]. NC-AFM measurements are performed with a well characterized system[16–18] where KPFM[19,20] measurements are performed simultaneously by applying an AC voltage of 1 V_{PP} amplitude and a frequency of 1.2 kHz added to the DC bias regulated to minimize electrostatic forces. In the KPFM measurements, the measured potential is relative to a reference potential being the tip potential. By simultaneously recording the NC-AFM and KPFM images, we are able to yield correct height information and identify different graphene sheet thicknesses[12] in a controlled (UHV) environment and beyond the spatial resolution attainable by (micro-)Raman spectroscopy with the risk of heating or even boiling confined hydration layers upon laser irradiation[21].

Address correspondence to Bollmann T.R.J., tbollman@uos.de

Calculations are performed using DFT[22,23] within the generalized gradient approximation (GGA) of the Perdew-Burke-Ernzerhof[24] parametrization with periodic boundary conditions using the Vienna ab-initio simulation package[25–27]. The projector augmented-wave (PAW) method along with a plane wave basis set with an energy cutoff at 425 eV is used. To calculate atomic and electronic structures, the Brillouin zone is sampled according to the MonkhorstPack[28] scheme with 4×4 k-points in periodical directions, combining the graphene 3×3 and $CaF_2(111)$ 2×2 super-cells with lattice constants of $a_{graphene}$ = 2.46 Å and $a_{CaF2(111)}$ = 3.86 Å respectively. To avoid spurious interactions between neighboring structures in a tetragonal super-cell, a vacuum layer of 17 Å is included in all non-periodic directions. The water density corresponds to 8.43 water molecules per nm^{-2}, slightly below the density of liquid water and in agreement with literature[29,30]. Structural relaxation is performed until the forces acting on each atom are less than 0.05 eV/Å. Molecular dynamics (MD) simulations are carried out at 300 K using the Nosè-Hoover thermostat[31,32] over 10 ps with 1 fs time steps. For the analysis of the atomic geometry and electronic properties, statistics are taken from 10 snapshots randomly chosen after equilibrium has been established for all situations investigated and described below.
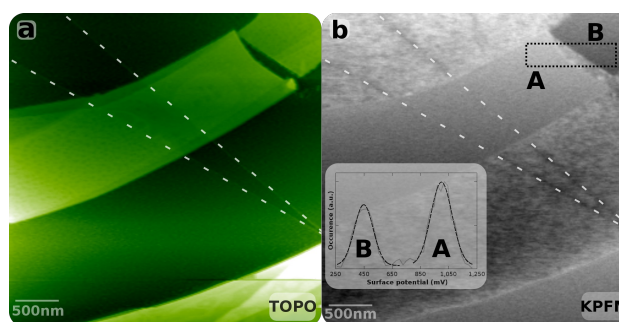
Figure 1: (color on-line) Topography (a) and local surface potential (b) image of few layer graphene flakes. Substrate steps are marked by (white) dashed lines both in (a) and (b). Graphene flakes A and B, in near vicinity of each other, show a strong difference in their local surface potential where the inset shows a fit of normal distributions to the local surface potential values found in the area enclosed by the dashed rectangle.

Results

To visualize the modification of the electronic properties of graphene, we image the graphene flakes topography by NC-AFM and the corresponding surface potential by KPFM as shown in Fig. 1. Triple layer F^- -Ca^{2+} -F^- substrate steps can be identified in both, topographic and KPFM images[33] . The contrast found between the few layer graphene flakes labeled A and B in Fig. 1(b), which are of similar height, can not be understood from their thickness (of about five layers), as only one, two and three layers of graphene can be discriminated in KPFM with reasonable contrast[12]. Note that the contrast distinguishing the thinnest graphene sheets from each other is about 110 mV[12,34] while the surface potential of flake B is lower by 550 mV than that of flake A.
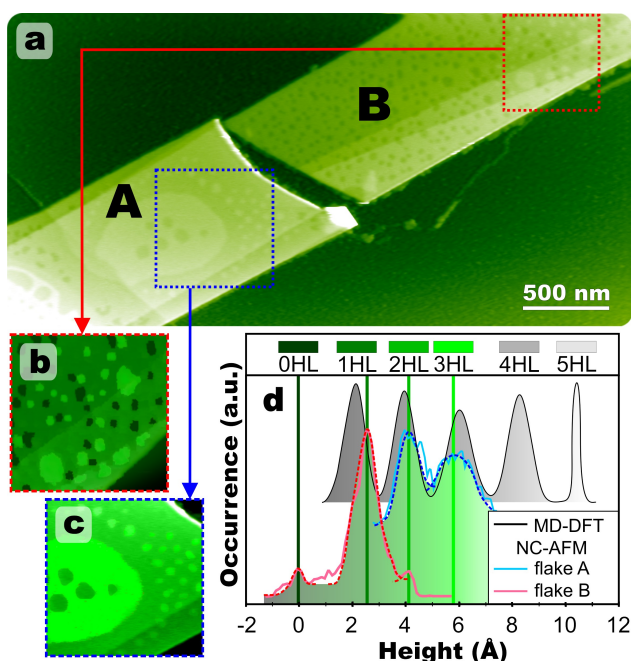
Figure 2: (color on-line) NC-AFM image (a) of two few layer graphene flakes, corresponding to the flakes labeled A and B in Fig. 1. From the height histograms of the Kuwahara filtered[34] areas marked in the corresponding red (b) and blue (c) height levels of the first three HLs (d) are identified. Experimental data is fitted by normal distributions and color-coded corresponding to images (b) and (c). Height levels marked by gray color are obtained from DFT calculations.

To investigate the mechanism responsible for this strong contrast, we investigate the topography of flakes A and B in detail as shown in Fig. 2(a). Mild annealing of the confined water layer to 400 K, results in a decay of HLs[12] and different height levels for the flakes shown in Fig. 2(a). By plotting the height distributions, of the corresponding dashed rectangles (Fig. 2(b-c)) in Fig. 2(d), we determine the heights of the individual HLs. Graphene flake A confines a full second HL and partially a third HL, whereas flake B in majority confines a partial first HL, with an areal coverage of 80±2%, with some second HL patches in the top right corner of Fig. 2(a). To understand the dependence of the surface potential on the number of HLs confined between graphene and substrate, we perform MD simulations of the system at RT where we vary the

number of confined HLs from none to five, with results shown in Figs. 2(d) and 3. The calculated structures reveal HL heights, determined from the graphene-substrate distance, in agreement with experimental observations as evident from Fig. 2(d). For the calculated structures, we obtain the charge density difference between the electronic density of the structure as a whole, as it is depicted in Fig. 3, in comparison to summing both freestanding graphene and freestanding slabs of $CaF_2(111)$ together with HLs present on-top. This allows us to directly see the redistribution of charge originating from the interaction between the hydration layers and graphene. As can be clearly seen from Fig. 3, in the first 2-3 HLs right below graphene, water molecules orient in such a manner that a net dipole is created drawing graphene's electrons slightly towards the adjacent HL. The strongly ionic CaF_2 substrate makes, apart from minor charge redistribution on the upper fluorite-layer, no significant contribution to graphene's electronic properties. We, therefore, conclude that the confined water layers do not (only) shield the interfacial charge at the substrate[10], but rather contribute to the electronic rearrangement whereas the substrate stays 'electroneutral'. The electronic contribution of the confined HLs to the graphene above, is determined by a Bader analysis[36] of the charge distribution, with results summarized in Fig. 4 where the reduction in free charge carrier density per unit cell (uc) is drawn for increasing number of HLs. For no HL present, we define the free charge carrier density of graphene to be zero. From this analysis, we find a decrease (increase) in electron (hole) density for graphene as the number of HLs increases. As the free charge carrier density within graphene is lowered under the influence of the highly electronegative oxygen atoms in water molecules, attracting electron density, the confined HLs effectively yield hole doping of graphene. This conclusion is in line with the observation of

increasing surface potential (brighter contrast) for decreasing graphene thickness as it is represented in Fig. 1(d) of Ref.12 . Since we determine from Fig. 3 that only the 2 to 3 HLs adjacent to graphene contribute to the electronic rearrangement, we expect an asymptotic behavior for the electron transfer as a function of confined HLs what is well in accordance with the DFT results shown in Fig. 4.

Discussion

mV between the graphene flakes A and B in Fig. 1, quantitatively shows the lower electron density of flake A compared to flake B. This decrease in the electron density stems from the thicker confined HLs present, as found to be about 2.5 ML of flake A from the topographic image in Fig. 2(a). The less decreased electron density for flake B, on the other hand, revealed by the more negative surface potential found in the KPFM image, arises from the smaller average thickness and the partial absence (20%) of Hls.

Figure 3: *(color on-line) MD snapshots of the atomic positions for n HLs confined by graphene and the CaF$_2$(111) substrate underneath (side view) with the electronic influx and outflux marked by blue and yellow respectively. The calculated electronic redistribution reveals the net dipole formation of the first three HLs below the graphene. Carbon (violet), oxygen (red), hydrogen (cyan), calcium (gray) and fluorine (green) atoms are marked.*

Because of the strong delocalization of electrons in graphene, the resulting homogeneous contrast in our KPFM measurements reflects the decrease in electron density for increasing confined HLs present, representing the more positive (hole doped) charge on the graphene. The contrast of 550

To quantitatively compare the doping observed in our experiments to the calculated free charge carrier density plotted in Fig. 4, we use a simple capacitor model[37] based on the approximation of graphene's density of states (DOS) being linear within close vicinity of the conical points[38] since the interaction

between HLs and graphene is weak, and the details of the bandstructure in the near vicinity of the K-point for FLG[39] do not come into play for the Fermi level shifts discussed here. Note that in our experimental setup the potential difference between the tip and the backside electrode of the insulating substrate is measured, which is for the system under investigation effectively dominated by the potential difference across the substrate and HL. The surface potential difference determined corresponds to a Fermi level shift[38] in the graphene flake being proportional to the density of free charge carriers at the Fermi-level (n_F) as:

$$\Delta n_F = \left(\frac{\delta E_F}{\hbar\, v_F} \right)^2 / \pi$$

where δE_F is the Fermi level shift and the Fermi velocity $\hbar v_F$ = 6.726 eVÅ [40,41]. Assuming the Fermi level shift determined between flakes A and B labeled in Fig. 1(b) of 550 mV, we determine a free charge carrier density increase of 2.1×10^{-3} carriers per Å^2. Applying the unit cell area of graphene (5.24 Å^2) this translates into 0.011 holes/uc, a similar value as one would expect from the extrapolation of the free charge carrier density and corresponding surface potential difference calculated in the graph shown in Fig. 4, where we estimated the average HL coverage as 0.8 ML and 2.5 ML from the analysis discussed above. Note that for an accurate estimate of the free charge carrier density, one should take the average coverage of the entire flake into account as well as the screening of the electrical field for larger numbers of graphene layers[42] . Our simple model predicts that the surface potential between a system without confined HLs in comparison to a system with one HL present is an order of magnitude larger than the decrease in surface
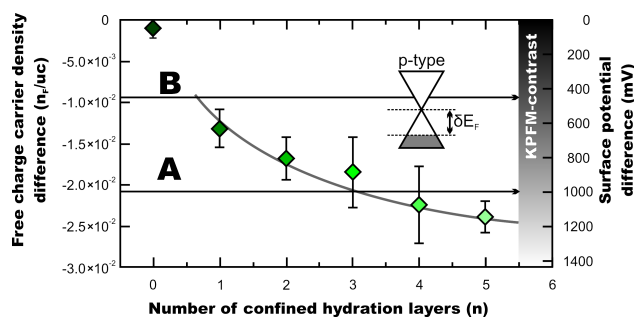
Figure 4: The decaying free charge carrier density of graphene for increasing number of confined HLs, representing the increase of holes (p-type doping) for increasing number of confined HLs. The gray line serves as a guide-to-the-eye for the asymptotic behavior for thick confined HLs. The calculated surface potential difference and corresponding contrast in KPFM imaging is shown at the right.

potential for incrementing confined HLs present, in agreement with experimental observations of confined water layers on mica[10]. The different HL heights present under the same flake do not correlate to KPFM images, although our resolution in KPFM is several tens of mV as we are able to discriminate the CaF$_2$(111) substrate ledges in KPFM[33] in Fig. 1(b). This uniform doping over the entire flake can however be easily understood from the free delocalized electrons present in graphene. In contrast to graphene on mica[10,13], we do not observe local doping where the edges of the water-free domains[12] serve as demarcations for the doping variations. This might very well result from the different behavior upon cleavage leaving more charge on the surface of mica compared to CaF$_2$(111).

Summary

In conclusion, we elucidate the processes of hole doping graphene by confined HLs by imaging the topography of HLs by NC-AFM and correlating this with surface potential data obtained by KPFM. The HLs that are confined upon mechanical exfoliation not only influence the mechanical properties of

graphene[12], but are also found to yield hole doping of graphene. By comparing the experimentally determined surface topography with MD-DFT calculations, we are able to identify different HLs and describe their electronic contribution to the graphene. The 2 to 3 HLs adjacent to the graphene turn out to be responsible for the hole doping of graphene by forming a net dipole drawing graphene's electrons slightly towards the HLs. HLs beyond this thickness do only marginally contribute to hole doping. Although this investigation has been performed on a specific substrate, namely $CaF_2(111)$, findings can be generalized, as the (hydrophilic) substrate is not involved in the electronic rearrangement. Making use of this doping mechanism in a controlled way by e.g. creating specific hydrophobic/hydrophilic substrate architectures, could be used to tailor graphene's electronic properties for future applications such as e.g. humidity sensors.

Acknowledgements

References

[1]   K.S. Novoselov, A.K. Geim, S.V. Morozov, D. Jiang, Y. Zhang, S.V. Dubonos, I.V. Grigorieva, and A.A. Firsov. Electric field effect in atomically thin carbon films. *Science* **2004**, 306, 666–669.

[2]   Dai-Ming Tang, Dmitry G Kvashnin, Sina Najmaei, Yoshio Bando, Koji Kimoto, Pekka Koskinen, Pulickel M Ajayan, Boris I Yakobson, Pavel B Sorokin, Jun Lou, and Dmitri Golberg. Nanomechanical cleavage of molybdenum disulphide atomic layers. *Nature Commun.* **2014**, 5,3631.

[3]   Ji-Eun Song, Taeg-Yeoung Ko, and Sun-Min Ryu. Raman spectroscopy study of annealing-induced effects on graphene prepared by micromechanical exfoliation. *Bulletin of the Korean Chemical Society* **2010**,31,2679–2682.

[4]   Ke Xu, Peigen Cao, and James R. Heath. Graphene visualizes the first water adlayers on mica at ambient conditions. *Science* **2010**, 329,1188–1191.

[5]   Peigen Cao, Ke Xu, Joseph O. Varghese, and James R. Heath. The microscopic structure of adsorbed water on hydrophobic surfaces under ambient conditions. *Nano Letters* **2011**, 11,5581–5586.

[6]   Kevin T. He, Joshua D. Wood, Gregory P. Doidge, Eric Pop, and Joseph W. Lyding. Scanning tunneling microscopy study and nanomanipulation of graphene-coated water on mica. *Nano Letters* **2012**, 12(6),2665–2672.

[7]   Hiroki Komurasaki, Takahiro Tsukamoto, Kenji Yamazaki, and Toshio Ogino. Layered structures of interfacial water and their effects on Raman spectra in graphene-on-sapphire systems. *The Journal of Physical Chemistry C* **2012**, 116(18),10084–10089.

[8]

Mi Jung Lee, Jin Sik Choi, Jin-Soo Kim, Ik-Su Byun, Duk Hyun Lee, Sunmin Ryu, Changgu Lee, and Bae Ho Park. Characteristics and effects of diffused water between graphene and a SiO_2 substrate. *Nano Research* **2012**, 5,710–717.

[9]

Nikolai Severin, Philipp Lange, Igor M. Sokolov, and Jürgen P. Rabe. Reversible dewetting of a molecularly thin fluid water film in a soft graphene/mica slit pore. *Nano Letters* **2012**,

12,774–779.

[10]   Jihye Shim, Chun Hung Lui, Taeg Yeoung Ko, Young-Jun Yu, Philip Kim, Tony F. Heinz, and Sunmin Ryu. Water-gated charge doping of graphene induced by mica substrates. *Nano Letters* **2012**, 12,648–654.

[11]

Albert Verdaguer, Juan Jose Segura, Laura Lopez-Mir, Guillaume Sauthier, and Jordi Fraxedas. Communication: Growing room temperature ice with graphene. *The Journal of Chemical Physics* **2013**, 138,121101.

[12]   M. Temmen, O. Ochedowski, M. Schleberger, M. Reichling, and T.R.J. Bollmann. Hydration layers trapped between graphene and a hydrophilic substrate. *New J. Phys.* **2014**, 16,053039, 2014.

[13]   Scott J. Goncher, Liuyan Zhao, Abhay N. Pasupathy, and George W. Flynn. Substrate level control of the local doping in graphene. *Nano Letters* **2013**, 13(4),1386–1392.

[14]   L. M. Malard, M. A. Pimenta, G. Dresselhaus, and M. S. Dresselhaus. Raman spectroscopy in graphene. *Physics Reports* **2009**, 473,51–87.

[15]   Andrea C. Ferrari and Denis M. Basko. Raman spectroscopy as a versatile tool for studying the properties of graphene. *Nature Nanotechnology* **2013**, 8,235–246.

[16]   J. Lübbe, L. Tröger, S. Torbrügge, R. Bechstein, C. Richter, A. Kühnle, and M. Reichling. Achieving high effective Q-factors in ultra-high vacuum dynamic force microscopy. *Meas. Sci. Technol.* **2010**, 21,125501.

[17]   J. Lübbe, L. Doering, and M. Reichling. Precise determination of force microscopy cantilever stiffness from dimensions and eigenfrequencies. *Meas. Sci. Technol.* **2012**, 23,045401.

[18]   J. Lübbe, M. Temmen, S. Rode, P. Rahe, A. Kühnle, and M. Reichling. Thermal noise limit for ultra-high vacuum noncontact atomic force microscopy. *Beilstein J. Nanotechnol.* **2013**, 4,32–

44.

[19]   M. Nonnenmacher, M. P. O'Boyle, and H. K. Wickramasinghe. Kelvin probe force microscopy. *Appl. Phys. Lett.* **1991**, 58,2921–2923.

[20]   J. M. R. Weaver and David W. Abraham. High resolution atomic force microscopy potentiometry. *J. Vac. Sci. Technol. B* **1991**, 9,1559–1561.

[21]   V.D. Frolov, P.A. Pivovarov, E.V. Zavedeev, A.A. Khomich, A.N. Grigorenko, and V.I. Konov. Laser-induced local profile transformation of multilayered graphene on a substrate. *Optics & Laser Technology* **2015**, 69, 34-38.

[22]   P Hohenberg and W Kohn. Inhomogeneous electron gas. *Phys. Rev* **1964**, 136(3B),B864–B871.

[23]   W Kohn and L J Sham. Self-consistent equations including exchange and correlation effects. *Phys. Rev.* **1965**, 140(4),A1133–A1138.

[24]   J P Perdew, K Burke, and M Ernzerhof. Generalized gradient approximation made simple. *Phys. Rev. Lett.* **1996**, 77(18),3865–3868.

[25]   G Kresse and J Hafner. Ab initio molecular dynamics for liquid metals. *Phys. Rev. B* **1993**, 47(1),558–561.

[26]   G Kresse and J Hafner. Ab initio molecular-dynamics simulation of the liquid-metal-amorphous-semiconductor transition in germanium. *Phys. Rev. B* **1994**, 49(20),14251–14269.

[27]   G. Kresse and J. Furthmüller. Efficient iterative schemes for ab initio total-energy calculations using a plane-wave basis set. *Phys. Rev. B* **1996**, 54,11169–11186.

[28]   Hendrik J. Monkhorst and James D. Pack. Special points for Brillouin-zone integrations. *Phys. Rev. B* **1976**, 13, 5188–5192.

[29]   Bernhard Reischl, Matthew Watkins, and Adam S. Foster. Free energy approaches for modeling atomic force microscopy in liquids. *Journal of Chemical Theory and Computation* **2013**, 9,600–608.

[30]   J. Moser, A. Verdaguer, D. Jimenez, A. Barreiro, and A. Bachtold. The environment of graphene

probed by electrostatic force microscopy. *Appl. Phys. Lett.* **2008**, 92, 123507.

[31]   Shuichi Nosè. A unified formulation of the constant temperature molecular dynamics methods. *J. Chem. Phys.* **1984**, 81(1),511–519, 1984.

[32]   William G. Hoover. Canonical dynamics: Equilibrium phase-space distributions. *Phys. Rev. A* **1985**, 31,1695–1697.

[33]   H. H. Pieper, C. Barth, and M. Reichling. Characterization of atomic step structures on CaF$_2$(111) by their electric potential. *Applied Physics Letters* **2012**, 101(5):051601.

[34]   T. Filleter, K. V. Emtsev, Th. Seyller, and R. Bennewitz. Local work function measurements of epitaxial graphene. *Appl. Phys. Lett.* **2008**, 93,133117.

[35]   John C. Russ. The Image Processing Handbook. CRC Press, Inc., Boca Raton, FL, USA, 5th edition, December **2006**.

[36]   Richard F W Bader. Atoms in molecules. Wiley Online Library, **1990**.

[37]   Feng Wang, Yuanbo Zhang, Chuanshan Tian, Caglar Girit, Alex Zettl, Michael Crommie, and Y. Ron Shen. Gate-Variable Optical Transitions in Graphene. *Science* **2008**, 320(5873),206–209.

[38]   G. Giovannetti, P. Khomyakov, G. Brocks, V. Karpan, J. van den Brink, and P. Kelly. Doping graphene with metal contacts. *Phys. Rev. Lett.* **2008**, 101,026803.

[39]   Sylvain Latil and Luc Henrard. Charge carriers in few-layer graphene films. *Phys. Rev. Lett.* **2006**, 97,036803.

[40]   A.K. Geim and K.S. Novoselov. The rise of graphene. *Nature Materials* **2007**, 6,183.

[41]   A. Bostwick, T. Ohta, T. Seyller, K. Horn, and E. Rotenberg. Quasiparticle dynamics in graphene. *Nature Physics* **2007**, 3,36.

[42]   D. Ziegler, P. Gava, J. Güttinger, F. Molitor, L. Wirtz, M. Lazzeri, A. M. Saitta, A. Stemmer, F. Mauri, and C. Stampfer. Variations in the work function of doped single- and few-layer graphene assessed by Kelvin probe force microscopy and density functional theory. *Phys. Rev. B* **2011**, 83, 235434.